JOURNAL OF CATALYSIS **134**, 678–690 (1992)

Nonparametric Determination of Reactivity Distributions from Isotopic Transient Kinetic Data

T. EDDY HOOST[1] AND JAMES G. GOODWIN, JR.[2]

Chemical and Petroleum Engineering Department, University of Pittsburgh, Pittsburgh, Pennsylvania 15261

Received April 24, 1991; revised November 1, 1991

This paper presents a new, rigorous approach for the nonparametric determination of catalytic reactivity distributions from *in situ* kinetic information obtained using steady-state isotopic transient kinetic analysis (SSITKA). The method is based on a constrained, standard Tikhonov regularization of Fredholm integral equations of the first kind. Results of the validation and application of this method for the analysis of synthetic and real (ruthenium-catalyzed CO hydrogenation) data are given. The method was compared to another nonparametric one that is based on an inverse Laplace transformation introduced by M. de Pontes, G. H. Yokomizo, and A. T. Bell (*J. Catal.* **104,** 147 (1987)) and was found to be less subjective and more exact, but computationally more demanding. For the new method, the effects of measurement noise and incorrect background selection on the recovery of reactivity distributions were also evaluated. It was shown that the new method could faithfully recover reactivity distributions even when reasonably small amounts of random noise were present. Similar recovery tests also showed that proper background selection would be critical for the determination of reliable reactivity spectra.

1. INTRODUCTION

Steady-state isotopic transient kinetic analysis (SSITKA) developed in large part by Happel (*1*) and Biloen (*2*) is beginning to be routinely applied in catalysis (*3–9*). In this method only the isotopic concentration of the catalyst's environment is changed, so that, in the absence of isotope effects, the ongoing steady-state reaction and the populations of reaction intermediates on the catalyst surface are not disturbed. Other transient methods (*10–13*) do not guarantee this preservation of the steady state. Thus, using these latter methods it is sometimes not clear whether the actual transient kinetic response has been obscured or complicated by extraneous phenomena, such as changes in surface coverage, induced by changes in pressure and/or flow rates. They are therefore not as suitable for quantifying steady-state kinetic behavior, even though they may still reveal important mechanistic information.

Depending on the reaction system under consideration, the analysis of transient responses to step changes in the isotopic content of the reaction feed varies from being rather complex (e.g., Fischer–Tropsch synthesis) to relatively straightforward. For irreversible, first-order reactions such as the methanation reaction, Happel *et al.* (*14*) and Biloen *et al.* (*15*) showed that the steady-state reaction rate can be expressed as

$$R_{ss} = N\bar{k}, \quad (1)$$

where N is the abundance in surface reaction intermediates, while their mean reactivity, $\bar{k}$, turns out to be the reciprocal of the integrated normalized response (i.e., the response time) to the isotopic step change; this integrated value is itself equal to the surface residence time of the isotopically marked element in the species being traced. Such data analysis, sometimes with additional assumptions, has been applied often to steady-state isotopic transients to arrive at coverages and average lifetimes of sur-

---

[1] Present address: Research Staff, Ford Motor Company, P.O. Box 2053, Dearborn, MI 48121.

[2] To whom correspondence should be addressed.

0021-9517/92 $3.00

face intermediates for a number of reactions (*3–9*).

For isotopic transient kinetic studies of the methanation reaction, Biloen (*2*) emphasized that the dynamic behavior of the reaction rate of the labeled reactant is

$$R(t) = Nke^{-kt} \qquad (2)$$

provided that the reaction steady state is not disturbed and the reactor is well-mixed. Based on Eq. (2), Scott and Phillips (*16, 17*) developed a six-parameter model to arrive at reactivity distributions for methanation in stopped-flow chromatography by summation of the activity of all the parallel, independent methanation sites; that is,

$$F(t) = R(t)/N = \int_0^\infty ke^{-kt}f(k)\,dk, \qquad (3)$$

where $f(k)$ is the reactivity distribution function for the active sites and $F(t)$ represents the normalized transient data. Soong *et al.* (*18*) later confirmed that the types of methanation sites work in parallel, even though it could not be distinguished if and how they might be connected. Although Scott (*16*) showed that he could satisfactorily recover his particular $f(k)$, the difficulty with his method is that it limits the distribution's shape to that of bimodal Gaussians. In addition, there are risks in using many-parameter models to fit inexact data that do not entirely obey the underlying model criteria because the extracted parameters and, consequently, their description of any phenomena may not be correct, even though the fit is good. These issues are pointed out because a priori it is not clear what form $f(k)$ has for a specific catalyst in a particular reaction environment. For the determination of $f(k)$ by the method of Scott, these concerns become even more important since the methanation sites react to perturbations of the steady state (*19*). In addition, the inherent integral nature of his reactor was also not addressed.

For isotopic transients obtained during the methanation reaction and assuming Eq. (3), de Pontes, Yokomizo, and Bell (*5*) (DYB) introduced a method based on a shortcut in an eigenfunction-based transformation technique devised by McWhirter and Pike (*20*) to arrive a posteriori at nonparametric reactivity distributions of the active methanation sites for their ruthenium catalysts and the nickel ones of Soong *et al.* (*18*). The use of nonparametric methods that do not assume a specific functional form for $f(k)$ is preferred over modeling if the problem at hand is not too ill posed due to excessive, random measurement noise. Even so, the DYB method in particular has certain compromises or weaknesses, some of which are inherent to McWhirter and Pike's technique. Thus, for example, only a few points at a time (four in Ref. (*5*)) are used in k-space to transform the data and assemble the reactivity distribution through "retracing." Stabilization of the transformation is based on certain postulates about $f(k)$ rather than on knowledge about $R(t)$. However, the physical nonnegativity requirement of $f(k)$ is not used to constrain the problem. Space restrictions prohibit a lengthy discussion; however, it should be noted that the aforementioned difficulties are essentially due to a nonoptimal use of information about the problem at hand. It might be expected, then, that a method that properly addresses them would improve the solution.

In this paper we describe a rigorous method to determine nonparametric reactivity distributions from isotopic transients obtained *in situ* during steady-state reaction. Our method (henceforth referred to as the T-F method) is based on a constrained, standard Tikhonov regularization of first-kind Fredholm integral equations (e.g., Eq. (3)) using a heuristic extension of an a posteriori rule devised by Butler *et al.* (*21*) to determine the optimal amount of smoothing needed during the transformation. The approach that Butler *et al.* (*21*) used to select the optimal amount of smoothing for the integral inversion has often been applied successfully in several other disciplines (*22–28*). Most other nonparametric methods that may be developed to estimate reactivity distributions do not have such an extensive record of practical use (*29*). Comparisons between the DYB and T-F methods are reported for the deconvolution of synthetic data derived from known bimodal reactivity distributions. The effects of several experimental difficulties—such as random noise and improper background subtraction—on the recovery of the reactivity distributions by the T-F method are also discussed. Extraction of nonparametric reactivity distributions will be illustrated with real data derived from isotopic transients obtained during steady-state methanation over a Ru/SiO_2 catalyst. Care must be taken in the assessment of experimentally obtained isotopic transients to ensure that extraneous effects such as gas-phase holdup, diffusion, or readsorption are negligible or properly accounted for in order for estimated reactivity distributions to be meaningful. Therefore, some critical issues in the evaluation of observed, experimental transient decays are also discussed.

2. METHODOLOGY

2.1. Numerical

For methanation in a well-mixed reactor, to arrive at Eq. (3) requires that each active site on the catalyst (i) obeys first-order kinetics and that these sites work (ii) in parallel and (iii) independently. Of these assumptions, Soong *et al.* (*18*) showed that the one requiring nonconnectivity is perhaps the weakest. Equation (3) can be compared to the general form of Fredholm integral equations of the first kind,

$$F(t) = \int_D h(t,k)f(k)\,dk, \qquad (4)$$

or simplified in terms of linear operators

$$F = Hf = Hf^0 + \varepsilon, \qquad (5)$$

where $h(t,k)$ is a nondegenerate kernel, $f^0(k)$ is the true distribution function in some convex domain D, and $f(k)$ is the estimate of $f^0(k)$ due to the presence of indeterminate error, ε, in the experimental data, $F(t)$. Thus, in our case, the kernel contains the inherent transient kinetic properties of each active site,

$$h(t,k) = ke^{-kt}, \qquad (6)$$

which is essentially Eq. (2) rewritten. In practice $F(t)$ is inexact because of random noise, and the problem of determining the density function $f^0(k)$ becomes ill posed—i.e., in case of excessive experimental noise there may be more than one solution, $f(k)$, that will satisfy the problem. Therefore, in the case of inexact data it becomes necessary to somehow stabilize the integral inversion to limit distortions of $f(k)$, the estimate of $f^0(k)$, due to measurement error. One popular way to do this is by the standard Tikhonov regularization (*30*), which constructs an objective functional that works to minimize the sum of squared residuals and, at the same time, attempts to control the smoothness of $f(k)$ through a so-called smoothing term. In particular, Tikhonov chose to rewrite the inversion problem as the minimization of the functional

$$\Phi_\alpha(f) = \|Hf - F\|^2 + \alpha\|f\|^2, \quad \alpha > 0, \qquad (7)$$

where α is a scalar smoothing parameter. It should be noted that for the standard inversion problem (i.e., no second term) there is severe undersmoothing—that is, large oscillations—in the recovered estimate f. Thus by having minimization of $\|f\|$ as part of the objective functional, one is provided (via proper selection of α) with a control on the variations in f during the transformation of the data. For a particular α, the directional derivative of $\Phi_\alpha(f)$ is

$$\nabla\phi_\alpha(f) = h^t(k)(Hf - F) + \alpha f(k), \qquad (8)$$

where $h(k)$, Hf, and F are vectors in $\mathbb{R}^n$ (n-dimension real space), n is the number of data points, and superscript t signifies the transposed matrix. When the directional derivative of $\Phi_\alpha(f)$ is equated to zero, the last equation can be rewritten for simplification to show that for a given α the minimum of the functional is located at the f_α that satisfies

$$f(k) \equiv \max(0, h^t(k)c), \quad (9)$$

$$(Hf - F) + \alpha c = 0, \quad (10)$$

where Eq. (9) includes the physical nonnegativity requirement for $f(k)$. In addition, $c \in \mathbb{R}^n$ is defined by Eq. (9) and is not a function of k. By defining the integral operator M with elements $M_{ij}(h^t c) \equiv \int_{h^t c>0} h_i(k)h_j(k)\,dk$ (*21*), which essentially operates on the domain or region where the integrand is positive, Eq. (10) can by simple substitution be rewritten to show that the minimum of $\Phi_\alpha(f)$ is located at

$$c = (M + \alpha I)^{-1}F, \quad (11)$$

where I is the identity matrix. Thus, in our implementation (Appendix A) to invert the Fredholm integral at a given α, the vector c identifies the minimum of the functional $\Phi_\alpha(f)$ and from this c, the distribution function $f_\alpha(k)$ can be found using the definition in Eq. (9).

The next problem is to specify a rule to find the optimal smoothing parameter that yields the best approximation of the true $f^0(k)$. A reasonable criterion is to use the discrepancy principle as Morozov suggested (*31*) and choose as optimal the α that minimizes the square error between f^0 and its current estimate f_α; i.e., minimize

$$\mathrm{SE}(\alpha) \equiv \int_D (f_\alpha(k) - f^0(k))^2\,dk = \|f_\alpha - f^0\|^2, \quad (12)$$

where SE has been expressed both in function and operator notation and D is the appropriate integral domain. Butler *et al.* (*21*) showed that by using the functional $\Phi_\alpha(f)$, given the fact that f^0 is not expected to contribute to the square error, minimization of the true square error between f^0 and its estimate f_α is similar to the minimization of the auxiliary function of the squared error

$$\mathrm{SE}^*(\alpha) \equiv \|f_\alpha - f^0\|^2 - \|f^0\|^2 = f_\alpha^t f_\alpha - 2f_\alpha^t f^0, \quad (13)$$

which through straightforward linear algebra was shown (*21*) to be equivalent to

$$\mathrm{SE}^*(\alpha) = F^tTMTF - 2F^tTF + 2\varepsilon^t c, \quad (14)$$

where $T \equiv (M + \alpha I)^{-1}$. Their treatment of the measurement error in the last term of the last equation resulted in a rule that locates the optimal α at the minimum of an approximation of SE*,

$$\mathrm{SE}^*(\alpha) \approx F^tTMTF - 2F^tTF + 2\sigma\sqrt{n}\|c\|, \quad (15)$$

where the scalar σ is the standard deviation in the experimental measurements. Thus, this smoothing rule does not depend on properties of the solution $f(k)$. Unfortunately, the last term in Eq. (15) estimates the contribution of the noise rather conservatively, which may often lead to oversmoothing.

Butler *et al.* (*21*) pointed out that in terms of the recovery of the shape of $f(k)$ oversmoothing is preferred to undersmoothing; even so, we found that for our kernel (Eq. (6)) the level of oversmoothing was unacceptable. Some tests showed that in our case in general the most faithful recovery occurred at α's several orders of magnitude smaller than the α_{opt} found using the smoothing rule by Butler *et al.* Several other authors (*22–25*) have also encountered this problem of excessive smoothing. In an application to obtain selectivity coefficient distributions from ion-exchange adsorption isotherms, Triay and Rundberg (*23*) through numerical experimentation noted that the actual optimal smoothing parameter was usually about one-tenth of the α_{opt} calculated by the rule of Butler *et al.* Accordingly, their modified smoothing rule contains an empirical factor of 0.1 applied to the optimal α of Butler *et al.* Earlier, Thigpen *et al.* (*22*) had arbitrarily used this one-tenth rule to recover retardation-time spectra from creep data, and they commented that an objective rule to locate the true α_{opt} was needed to better warrant proper interpretation of distribution functions extracted from experimental data.

We decided that it might be possible to get a more reasonable estimate of the contribution of the experimental noise to the square error. The last term in the rule of Butler *et al.* (Eq. (15)) was restored to the more general $2\varepsilon^t c$. Then, whenever a solution $f_\alpha(k)$ had been determined for a given smoothing parameter by minimization of the constrained form of the functional in Eq. (7), we evaluated the right-hand side of Eq. (4) to observe the $F_\alpha(t)$ represented by this f_α. From this feedback, ε was estimated by ε_α, the vector difference between F and F_α. That is, our new smoothing rule is

$$SE^*(\alpha) \approx F^tTMTF - 2F^tTF + 2\varepsilon_\alpha^t c, \quad (16)$$

where $\varepsilon_\alpha = F - F_\alpha$, and $F_\alpha = Hf_\alpha$. It should be noted that, since there is an a posteriori estimate of $\|\varepsilon\|$ (i.e., $\sigma\sqrt{n}$), it may not be necessary to rely entirely on ε_α to assess the contribution of ε to SE*. Rather, it would be necessary to estimate only φ, the angle between ε and c, using ε_α, the α-estimate of the experimental error. That is,

$$SE^*(\alpha) \approx F^tTMTF - 2F^tTF + 2\sigma\sqrt{n}(\varepsilon_\alpha^t c/\|\varepsilon_\alpha\|). \quad (17)$$

Thus, in essence, at every α-iteration this rule would attempt to estimate the current direction of the indeterminate error before evaluating the angle of the inner product $\|\varepsilon\|\,\|c\| \cos \varphi$. Butler *et al.* (*21*), on the other hand, conservatively fixed $\cos \varphi$ at 1 so that their estimate of the contribution of the indeterminate error to SE* would be as large as possible.

The rule of Eq. (16) estimates both the direction and the size of the error using the current f_α to fit the data and does not compel the experimenter to rely on a separate method to determine $\|\varepsilon\|$. Heuristically, it is also clear that if the f_α estimate is poor, this will lead to a poor fit of the data resulting in large $\|\varepsilon\|$, which in turn, through Eq. (16), would tend to increase the value of SE*, the auxiliary function of the squared error. Several numerical tests have shown that of the several forms of Eq. (14) that were considered, the rule of Eq. (16) was the most adequate one for Eq. (6); that is, the most faithful recovery of the reactivity distribution coincided with the α_{opt} calculated from this new rule. Algorithmic details of the implementation of our method are in Appendix A.

Compared to the T-F method, the DYB method is somewhat indirect (see Appendix B). For that method the problem is viewed as having the Laplace kernel

$$h(t,k) = e^{-kt}, \quad (18)$$

and, using McWhirter and Pike's (*20*) transformation technique for Laplace-like kernels, Eq. (4) is solved for $kf(k)$. Thus to determine $f(k)$, this solution must be divided by k. The DYB method basically reduces the problem to a multiple regression (*5*).

It was convenient to implement the DYB method in a Lotus 123 worksheet using macro commands. Using 8-digit precision in floating-point arithmetic, it was run on a 12-MHz AT-bus computer equipped with a math coprocessor. Since the T-F method is computationally more demanding, it was programmed in C (MIPS cc under Ultrix-32 3.1D) and, using 16-digit precision, the optimized code was executed on RISC-based workstations (DECstation 2100).

2.2. *Experimental*

Details on the preparation procedure of the catalyst have been described elsewhere (it is catalyst K00 in Ref. (*36*)). In short, it was a chlorine-free, 3 wt% Ru/SiO_2 catalyst, which had been reduced in hydrogen at 400°C.

To arrive at reactivity distributions it is critical to properly acquire the steady-state isotopic transients. After *in situ* H_2 reduction at 400°C, isotopic methanation transients of the carbon were measured during steady-state CO hydrogenation over the catalyst, using a quartz, tubular fixed-bed microreactor (3-mm i.d.) differentially operated at 215°C, ca. 120 kPa, and a H_2/CO flow of 30/10 ml/min. The space velocity through the 60-mg, porous catalyst bed was maintained at about 80 s^{-1}. The ^{12}CO gas contained a 5.15% trace of argon. After the isotopic switch, $(^{12}CO + Ar_{trace}) + H_2//^{13}CO$

+ H_2, the effluent was continuously mass-analyzed (quadrupolar Extrel) to obtain the isotopic-transient decays. Further experimental details are described elsewhere (*37*).

In a recent paper Happel *et al.* (*38*) have rightly expressed concerns about what they perceived as the sometimes inappropriate analysis of steady-state isotopic transients obtained using plug-flow reactors. They emphasized that, in general, transients obtained using plug-flow reactors, even when operated at differential conversion, cannot be treated with formalisms derived for well-mixed reactors (CSTR's). In this study, a plug-flow reactor was used, and the resulting transient data were analyzed with expressions similar to those derived for well-mixed reactors because the system could be viewed as approximately gradientless. Thus, the reaction was maintained at differential conversion levels. Since we also used a differential catalyst bed, it is clear that in the differential equation system describing the mass balances of the reacting species, derivatives with respect to the axial position in the reacting bed can be disregarded.

For our reaction system the differential-bed approximation was valid because the space velocity was so high that the average contact time for the flow with the reacting bed (bed lengths of ca. 1.0 cm) was less than 1/80 s which is much shorter than any of the surface residence times measured. Furthermore, the effect of reactor dead space can be effectively removed because the presence of a trace amount of the inert Ar in one of the streams to be switched allowed us to measure the gas-phase holdup (τ^*_{Ar}) and to account for the delay time (induced by the dead space) between the switch and the onset of the transients. Thus, in our system, no delay was observed between the onsets of the Ar and methane transient decays. The gas-phase holdup measured using Ar was typically about 3 s. Since it can be assumed that the surface lifetime of irreversibly adsorbed CO is short (*39–41*), the gas-phase holdup can be subtracted from the decay time of methane ($\tau^*_{\mathrm{CH_4}}$) to determine the average surface residence time of the CH_x species terminating as methane ($\tau_{\mathrm{CH_4}}$).

For subsequent deconvolution of methane transients using Eq. (3), it is also necessary to remove the effect of the gas-phase holdup on the shape of these transients, especially when the flight time is considerable compared to the methane decay time. Recently, using Laplace transfer functions, Nwalor (*42*) showed that for gradientless systems the true reaction transient F of a product species, corrected for gas-phase holdup (τ^*_{Ar}), can be extracted from the overall transient decay as

$$F(t) = F^*(t) + \tau^*_{\mathrm{Ar}}(dF^*(t)/dt), \quad (19)$$

where F^* is the observed isotopic transient decay. Since the surface holdup for methane was relatively short, Nwalor's method was used to correct observed methane transients before the transformation to extract $f(k)$.

3. RESULTS AND DISCUSSION

3.1. The T–F Method

To test the precision of the T-F method, its effectiveness in recovering synthetic, Gaussian reactivity distributions was evaluated. The original, synthetic bimodal Gaussian distribution, $g_1(k)$, in Fig. 1 (solid line) has its peaks centered at $k = 0.03$ and $0.1\ \mathrm{s}^{-1}$ and both have a standard deviation of $0.01\ \mathrm{s}^{-1}$. This would correspond to two equally sized pools of active sites with average reactivities of 0.03 and $0.1\ \mathrm{s}^{-1}$. Using Eq. (4) with the kernel in Eq. (6), a direct forward transformation was applied to this bimodal Gaussian to yield a synthetic transient consisting of 40 points on the time interval [0–60 s]. Using a random-number generator, noise was added to this "exact" transient, $G_1(t)$, at different relative standard deviations (σ_{rel}). Subsequently, the algorithm described in Appendix A was used with the rule of Eq. (16) to assess the quality of the T-F recoveries of the original g_1 from these synthetic transients.

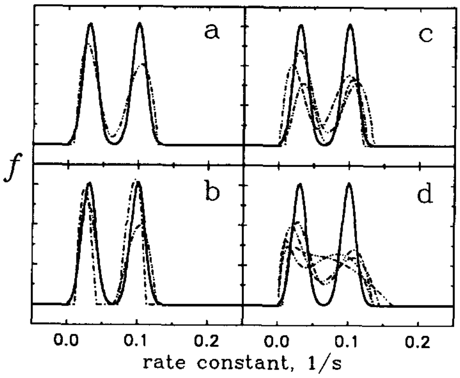

FIG. 1. Effect of random measurement noise on T-F recoveries (dot–dash lines) of bimodal Gaussian (solid lines); see text. Added noise ($\sigma_{\rm rel}$): (a) none, (b) 2.5%, (c) 5%, and (d) 10%.

Figure 1a shows that the recovery using the exact transient is quite satisfactory. The peak locations are estimated successfully but the peak widths of the T-F estimate are slightly broader, indicating that the solution is somewhat oversmoothed. However, the relative areas under the low- and high-activity peaks of the recovered distribution are 49 and 51%, respectively, which indicates that the average fraction of each pool of active sites is estimated accurately despite a modest level of oversmoothing.

Figures 1b, 1c, and 1d each show some typical T-F recoveries of g_1, the original distribution, when different levels of random noise ($\sigma_{\rm rel}$ = 2.5, 5, and 10% of $G(t)$, respectively) were added to the exact transient to simulate the effects of indeterminate measurement error. For each level of random noise several synthetic transients were created and deconvoluted. Thus, Fig. 1 shows that as the indeterminate error in the measurement of the transient increases the peak width of the recovered distribution increases. This peak broadening happens because in the presence of considerable noise more smoothing is needed to stabilize the integral inversion and prevent the problem from becoming too ill-posed. For small amounts of random noise (Fig. 1b) the family of T-F recoveries remains in a narrow band; but as the level of noise becomes considerable, the T-F solutions for a given $\sigma_{\rm rel}$ can become very dissimilar and may eventually in some cases become seriously distorted as can be seen in Fig. 1d.

Since due to experimental complications it is not always trivial to categorically determine the background of an isotopic transient, the effect of incorrect background selection on the quality of T-F recoveries of reactivity distributions has also been considered. In order to do so, synthetic transients were created from the exact normalized transient, G_1, where the background for the new normalized transients was selected with respect to $G_1(60)$ according to

$$F(t) = \frac{G_1(t) - (B/100)G_1(60)}{G_1(0) - (B/100)G_1(60)} * G_1(0), \quad (20)$$

where B is the percentage deviation for the background of the new transient with respect to $G_1(60)$. To illustrate the differences in these new transients they have been presented on a semilogarithmic basis in Fig. 2.

The T-F solutions using the transients shown in Fig. 2 are depicted in Fig. 3. From this figure it can be seen that modest under/overestimation of the isotopic transient's background does not appear to lead to serious distortions of the T-F estimates of g_1

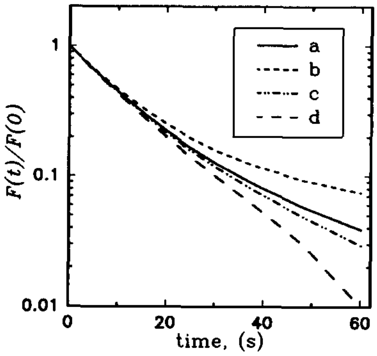

FIG. 2. Background selections for transients from bimodal Gaussians; see text. Specification w.r.t. $G_1(60)$: (a) correct, (b) −100%, (c) +25%, and (d) +75%.

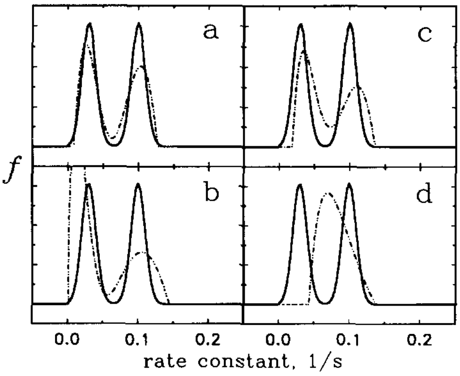

FIG. 3. Effect of incorrect background estimation on T-F recoveries (dot–dash lines) of bimodal Gaussian (solid lines); see text. Background specification w.r.t. $G_1(60)$: (a) correct, (b) -100%, (c) $+25\%$, and (d) $+75\%$.

(Fig. 3c). On the other hand, poor background estimation leads to severe distortions (Figs. 3b and 3d) in the T-F estimates, and especially gross underestimations may quickly lead to nonrepresentative recoveries of reactivity distributions.

The T-F method was also used to attempt to recover a bimodal Guassian reactivity distribution function for which the peak shapes were not similar. This bimodal Gaussian, $g_2(k)$, is shown in Fig. 4 and has its peaks located at 0.012 and 0.082 s^{-1}, with standard deviations of 0.002 and 0.015 s^{-1}, respectively. Such a distribution would correspond to a situation in which the low- and high-activity pools would each comprise 50% of the total number of active sites. The distribution g_2 was then integrated according to Eq. (4) using the kernel of Eq. (6) to arrive at the "exact" transient, $G_2(t)$, to which different levels of random noise could be added.

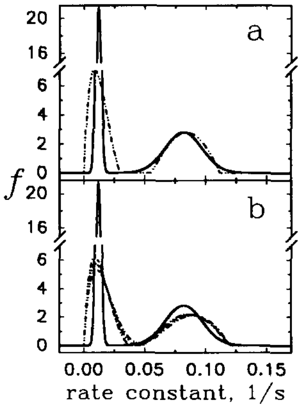

FIG. 4. T-F recovery (dot–dash) of mixed-band, bimodal Gaussian (solid): (a) no added noise; (b) 2.5% random noise. See text for details.

TABLE 1

Comparison of Peak Characteristics of Nonparametric Estimates of the Mixed-Band Bimodal Gaussian

Method	$\bar{k}_1$ (s^{-1})	x_1	$\bar{k}_2$ (s^{-1})	x_2
Original Gaussian	0.012	0.50	0.082	0.50
T–F method	0.012	0.54	0.084	0.46
Self-consistent DYB	0.021	0.54	0.075	0.46
Biased DYB method	0.016	0.47	0.070	0.53

Figure 4a shows the recovery of the exact transient G_2 by the T-F method. Figure 4b shows that reasonably low levels of added random noise ($\sigma_{rel} = 2.5\%$) in the transient again did not seriously affect the T-F estimation of $g_2(k)$. As can be seen in Table 1 the peaks in the original reactivity spectrum were located quite accurately as was the relative area of each peak (x). For the exact recovery (Fig. 4a), the shape of the recovered high-activity peak is quite faithful but the recovered low-activity peak shows considerable broadening because of too much smoothing. This broadening of the narrow peak occurs as a natural side effect of the regularization approach. That is, when trying to recover a mixed-band spectrum with very narrow and very wide bands, the tendency is for regularization methods to oversmooth the narrow bands. This happens because narrow bands occupy a relatively small domain so that the contribution of the much broader (smoother) bands to the regularization process will dominate since the latter require more smoothing for their description. Of course, alternatively,

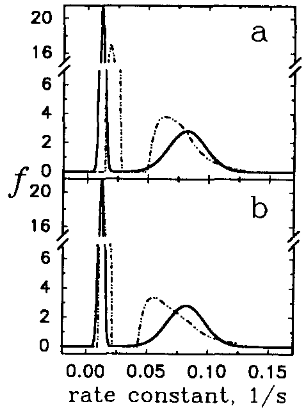

FIG. 5. Exact DYB recoveries (dot–dash) of mixed-band, bimodal Gaussian (solid): (a) "self-consistent" DYB estimate; (b) "biased" DYB estimate. See text for details.

mixed-band spectra may be addressed with nonsmoothing, nonparametric methods, but it should be kept in mind that for such non-regularization methods, the transformation often becomes much less stable (*29*).

3.2. Comparison of the T–F and DYB Methods

To compare the effectiveness of the T-F and DYB methods in determining nonparametric estimates of reactivity distributions, their accuracy in recovering a known bimodal Gaussian distribution $g_2(k)$ described earlier was tested. Figure 4a shows the T-F recovery using the exact transient $G_2(t)$, and Fig. 5 shows exact DYB recoveries. As explained by de Pontes *et al.* (*5*), the nonparametric DYB method is valid for $\|\varepsilon\| \leq 0.02$, where at the same time $\|\varepsilon\|$ may also be used to estimate the parameter $\omega_{\max}$, which dictates the spacing for sets of k in the reactivity domain (see Appendix B). Since for the exact transient $\|\varepsilon\|$ is essentially zero, the approach to assemble the recovery in Fig. 5a was to choose a $\omega_{\max}$ to space the values of k and then to calculate an average $\|\varepsilon_\omega\|$ from the fits of the sets of solutions (corresponding to the different sets of k) to the transient G_2. This procedure was then iterated until

$$\|\varepsilon_\omega\| - \sqrt{\pi/\cosh(\pi\omega_{\max})} < 10^{-3}. \qquad (21)$$

This approach, which essentially tries to control the proper spacing for the sets of k based on a current estimate of the error, is referred to as the "self-consistent" DYB method.

Figure 5a shows that the estimate using the self-consistent DYB approach is not as faithful as the one obtained by the T-F method. On the other hand, even though the high-activity peak is seriously skewed, this DYB recovery seems to have the correct amount of smoothness. Table 1 shows that although the relative fractions of the area under the peaks were estimated quite reasonably, the estimation of the average reactivity of these peaks cannot be considered satisfactory.

It is estimated that depending on certain run parameters the T-F calculation may take roughly 500–1000 times longer than the DYB inversion. Since the DYB method is computationally far less demanding than the T-F one, it was investigated to see if the former method could in fact recover distributions faithfully, perhaps at other values of $\omega_{\max}$. That is, the possibility was considered that our criterion for selecting $\omega_{\max}$ (Eq. (21)) may not lead to optimum error estimation. It was believed that if the DYB method could indeed accurately recover reactivity distributions at some other $\omega_{\max}$ value, then a new criterion could possibly be formulated to select this optimum condition. The DYB inversion was, therefore, also done at other values of $\omega_{\max}$. In particular, for one DYB recovery, the choice of $\omega_{\max}$ was biased to match the maximum of the low-activity peak of the recovery with the one of the original distribution. This DYB recovery is shown in Fig. 5b and is called the "biased" DYB estimate.

The biased DYB estimate indicates that the DYB method was not able to determine a satisfactory recovery of the original distribution using the exact transient (without any added noise). Table 1 shows, however, that the average fractions of the pools were still reasonably estimated. Figure 5b shows that recovery of the shape of the low-activity peak is excellent but that the underestimation of the location of the high-activity peak in the reactivity spectrum has become even more serious than in the case of the self-consistent DYB estimate.

The comparison of the DYB and T-F methods shows that because of the aforementioned improvements, the latter one is an important alternative of estimating reactivity spectra when the computational cost can be tolerated. It should be pointed out that the effectiveness of smoothing rules such as the heuristic one of Eq. (16), for a given first-kind Fredholm problem, will be at least partially related to the convergence rate of Morozov's discrepancy principle (*32*). That is, while smoothing rules based on Morozov's principle have been successful in many instances (*22–28*), Morozov's principle does not lead to optimal convergence rates (*33*). It may be expected that smoothing rules based on more adequate discrepancy principles such as that of Gfrerer (*33*) would be more effective in solving regularization problems (especially those with "difficult" kernels), but at the cost of greater computational complexity (*34*, *35*).

3.3. SSITKA of Methanation over Ru/SiO$_2$

The nonparametric T-F method was applied to determine the reactivity distribution of methanation over a 3 wt% Ru/M5-SiO$_2$ catalyst during Fischer–Tropsch reaction at the operating conditions mentioned in the Experimental section. As mentioned there, care was taken to remove the effect of gas-phase holdup from the observed isotopic transient of methane. At the prevailing reaction conditions, steady-state product analysis showed that the methane selectivity was 49.1% and that the methanation rate was 2.5 μmol/g s. In addition, SSITKA revealed that the methane-bound surface carbon spent an average of 4.2 s on the catalyst surface in a steady-state abundance (N_{CH_4}) of 9.4 μmol/g, which would correspond to a coverage of about 8.6% of the surface Ru atoms (based on static hydrogen chemisorption (*36*)).

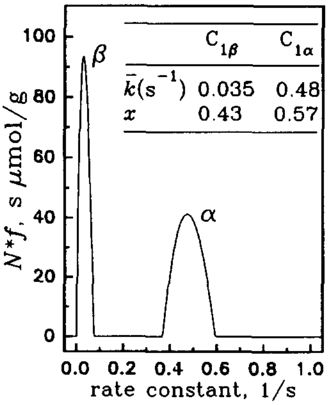

FIG. 6. Reactivity distribution obtained by SSITKA of methane-destined carbon during FTS over a 3 wt% Ru/M5-SiO$_2$ catalyst at 215°C, 120 kPa and H$_2$/CO = 3.

Using an arbitrary multiple regression with a sum of four exponentials, the average noise in the measurement of the transient was estimated at 2.2% with respect to the signal. As discussed earlier, the nonparametric T-F method may be expected to result in reasonable estimates of f^0 for such low levels of experimental noise. To solve the integral inversion in a reasonable amount of time, for the actual transformation 36 representative data points of the gas phase-corrected isotopic transient were used to obtain 201 points logarithmically spaced in the interval $k \in [0.005, 10 \text{ s}^{-1}]$.

The result of the calculation is given in Fig. 6, where the reactivity spectrum has been rescaled to reflect that the absolute abundance of methane-destined surface carbon is N. As mentioned before, the smoothness of the T-F estimate is a direct consequence of the regularization approach and any random experimental error would be primarily reflected as uncertainty about peak locations of the true reactivity function. For the current isotopic transient, such uncertainty is expected to be modest since the noise in the transient measurements is estimated to be small (see Fig. 1). From the reactivity spectrum in Fig. 6, two pools of active carbon can be distinguished and, as is typical (*5, 18*), they are assigned to a highly active α carbon ($C_{1\alpha}$) and a less active β form ($C_{1\beta}$). The figure also shows that at the prevailing reaction conditions the relative size (x) of the methane-destined $C_{1\alpha}$ pool was somewhat larger than that of $C_{1\beta}$ with CH_4 being produced on average about 14 times faster from $C_{1\alpha}$ than from $C_{1\beta}$. The T-F estimate of the reactivity spectrum is qualitatively similar to the DYB estimate by de Pontes *et al.* (*5*), who studied the methanation reaction over Ru/SiO_2 at much milder reaction conditions, and is in agreement with other studies that have established that there are two active surface carbon pools involved in the formation of methane (*43–46*).

4. CONCLUSIONS

A new method to extract nonparametric estimates of pseudo-first-order rate constant distributions from *in situ* isotopic transient kinetic data (the T-F method) has been presented and validated. It was shown that the method based on Tikhonov regularization could faithfully recover reactivity distributions even when reasonably small amounts of random noise were present. Similar recovery tests also showed that proper background selection is critical for the determination of reliable reactivity spectra. It was shown that in the case of mixed-band spectra containing very narrow and very wide bands, the narrow ones may suffer excessive oversmoothing. A comparison of the T-F method to the nonparametric method of de Pontes *et al.* (*5*) showed that the new method in general can recover reactivity distribution functions more reliably but at a significantly greater computational expense. The T-F method was demonstrated using a gas-phase-corrected isotopic transient of methane obtained at differential reaction conditions during CO hydrogenation over a 3 wt% Ru/SiO_2 catalyst. The resulting reactivity spectrum revealed two pools of active surface carbon, consistent with previous results of others.

APPENDIX A

The constrained search technique used here to determine $f_\alpha(k)$ at a given α from Eq. (7) is very similar to that of Butler *et al.* (*21*), but there are some important differences. It is basically a *quasi*-Newton method (*47*) to minimize the quadratic functional

$$\psi = 0.5c^t(M + \alpha I)c - c^tF \quad \text{(A1)}$$

with derivatives

$$\psi'(c) = (M + \alpha I)c - F \quad \text{(A2)}$$

and

$$\psi''(c) = (M + \alpha I), \quad \text{(A3)}$$

which represents the transformation problem at hand.

Iterations are according to

$$c_{i+1} = c_i - \delta\Delta, \quad \text{(A4)}$$

where the search direction is either

$$\Delta = (\psi'')^{-1}\psi' \quad \text{(A5)}$$

or, as suggested by Butler *et al.* (*21*),

$$\Delta = (M + \lambda I)^{-1}\psi' \quad \text{(A6)}$$

when α is small. $\lambda > 0$ is fixed to allow an estimate of the search direction when inversion of ψ'' is too difficult (*21*). The optimal step size δ is determined by a line search (*48*) along the direction Δ. The Newton search is typically continued until

$$\sigma_{\text{tol}} \equiv \frac{\|(M + \alpha I)c - F\|}{\|F\|} \leq 10^{-6}. \quad \text{(A7)}$$

Using this technique, convergence can become extremely slow, particularly if α is small (*21*). When this problem is encountered, the Newton search is terminated after about 150 iterations, provided that σ_{tol} is small.

The new rule in Eq. (16) is used to determine the proper level of smoothing for the integral transformation. Since the SE* function is convex, a logarithmic golden-section search (*49*) is used to locate the α_{opt} that minimizes it. The search for α_{opt} is stopped when the interval of uncertainty for $\log_{10} \alpha$ is less than 0.1.

APPENDIX B

For completeness, the essential equations necessary for implementing the DYB method are repeated here from Ref. (*5*) using our notation. Equation (3) can be rewritten in the form of a least-squares multiple regression

$$R(t) = \sum_{m=1}^{M} a_m e^{-k_m t}, \qquad \text{(B1)}$$

where M is set to 4. The a_m are the regression coefficients that contain the estimate, $f(k)$, of the reactivity distribution function according to

$$a_m = \frac{\pi}{\omega_{\max}} N k_m^2 f(k_m), \qquad \text{(B2)}$$

where N is the abundance of surface intermediates. The k_m are related by

$$k_{m+1} = k_1 e^{m\pi/\omega_{\max}}, \qquad \text{(B3)}$$

and the distribution can be assembled by retracing using different, arbitrary values of k_1. The spacing for each set of k_m is controlled by $\omega_{\max}$, which may be found from an estimate of the measurement error as

$$\|\varepsilon\| \approx \sqrt{\pi/\cosh(\pi\omega_{\max})}. \qquad \text{(B4)}$$

The method requires that $\|\varepsilon\| \leq 0.02$ be satisfied, and ε can be estimated by $\sigma\sqrt{n}$.

ACKNOWLEDGMENTS

The work presented here was financially supported by the National Science Foundation (Grant CBT-8715541). The Lotus worksheet used for the DYB method was implemented by Professor John U. Nwalor (current address is Department of Chemical Engineering, University of Lagos, Nigeria).

REFERENCES

1. Happel, J., *Chem. Eng. Sci.* **33,** 1567 (1978).
2. Biloen, P., *J. Mol. Catal.* **21,** 17 (1983).
3. Zhang, X., and Biloen, P., *J. Catal.* **98,** 468 (1986).
4. Stockwell, D. M., and Bennett, C. O., *J. Catal.* **110,** 354 (1988).
5. de Pontes, M., Yokomizo, G. H., and Bell, A. T., *J. Catal.* **104,** 147 (1987).
6. Mirodatos, C., Dalmon, J. A., and Martin, G. A., *J. Catal.* **105,** 405 (1987).
7. Nwalor, J. U., Goodwin, J. G., Jr., and Biloen, P., *J. Catal.* **117,** 121 (1989).
8. Peil, K., Goodwin, J. G., Jr., and Marcelin, G., *J. Phys. Chem.* **93,** 5977 (1989).
9. Mims, C. A., McCandlish, L. E., and Melchior, M. T., *Catal. Lett.* **1,** 121 (1988).
10. Parravano, G., *Catal. Rev.* **3,** 207 (1969).
11. Kobayishi, H., and Kobayishi, M., *Catal. Rev.-Sci. Eng.* **10,** 139 (1974).
12. Bennett, C. O., *Catal. Rev.-Sci. Eng.* **13,** 121 (1976).
13. Gleaves, J. T., Ebner, J. R., and Mills, P. L., *Stud. Surf. Sci. Catal.* **38,** 633 (1988).
14. Happel, J., Suzuki, I., Kokayeff, P., and Fthenakis, V., *J. Catal.* **65,** 59 (1980).
15. Biloen, P., Helle, J. N., van den Berg, F. G. A., and Sachtler, W. M. H., *J. Catal.* **81,** 450 (1980).
16. Scott, K. F., *J. Chem. Soc. Faraday 1* **76,** 2065 (1980).
17. Scott, K. F., and Phillips, C. S. G., *J. Chromatogr. Sci.* **21,** 125 (1983).
18. Soong, Y., Krishna, K., and Biloen, P., *J. Catal.* **97,** 330 (1986).
19. Cant, N. W., and Bell, A. T., *J. Catal.* **73,** 257 (1982).
20. McWhirter, J. G., and Pike, E. R., *J. Phys. A: Math. Gen.* **11,** 1729 (1978).
21. Butler, J. P., Reeds, J. A., and Dawson, S. V., *SIAM J. Numer. Anal.* **18,** 381 (1981).
22. Thigpen, L., Hedstrom, G. W., and Bonner, B. P., *Trans. ASME, Ser. E* **50,** 361 (1983).
23. Triay, I. R., and Rundberg, R. S., *J. Phys. Chem.* **91,** 5269 (1987).
24. Triay, I. R., and Rundberg, R. S., *Zeolites* **9,** 217 (1989).
25. Tyler, B. J., Castner, D. G., and Ratner, B. D., *J. Vac. Sci. Technol. A* **7,** 1646 (1989).
26. Munn, K., and Smith, D. M., *J. Colloid Interface Sci.* **119,** 117 (1987).
27. Gallegos, D. P., Munn, K., Smith, D. M., and Stermer, D. L., *J. Colloid Interface Sci.* **119,** 127 (1987).
28. Gallegos, D. P., and Smith, D. M., *J. Colloid Interface Sci.* **122,** 143 (1988).
29. Thomson, D. J., *Proc. IEEE* **70,** 1055 (1982).
30. Tikhonov, A. N., and Arsenin, V. Y., "Solution of Ill-Posed Problems." Wiley, New York, 1977.
31. Morozov, V. A., *USSR Comput. Math. Math. Phys.* **8,** 63 (1966).
32. Groetsch, C. W., *in* "Improperly Posed Problems and Their Numerical Treatment" (G. Hämmerlin and K. H. Hoffmann, Eds.). Birkhäuser, Basel, 1983.
33. Gfrerer, H., *Math. Comput.* **49,** 507 (1987).

34. Neubauer, A., *Computing* **39,** 43 (1987).

35. Neubauer, A., *SIAM J. Numer. Anal.* **25,** 1313 (1988).

36. Hoost, T. E., and Goodwin, J. G., Jr., *J. Catal.* **130,** 283 (1991).

37. Hoost, T. E., Ph.D. Dissertation, University of Pittsburgh, PA, 1991.

38. Happel, J., Walter, E., and Lecourtier, Y., *J. Catal.* **123,** 12 (1990).

39. Winslow, P., and Bell, A. T., *J. Catal.* **86,** 158 (1984).

40. Winslow, P., and Bell, A. T., *J. Catal.* **91,** 142 (1985).

41. Winslow, P., and Bell, A. T., *J. Catal.* **94,** 385 (1985).

42. Nwalor, J. U., Ph.D. Dissertation, University of Pittsburgh, PA, 1988.

43. McCarty, J. G., and Wise, H., *J. Catal.* **57,** 406 (1979).

44. Hayes, R. E., Ward, K. J., and Hayes, K. E., *Appl. Catal.* **20,** 123 (1986).

45. Yokomizo, G. H., and Bell, A. T., *J. Catal.* **119,** 467 (1989).

46. Siddall, J. H., Miller, M. L., and Delgass, W. N., *Chem. Eng. Commun.* **83,** 261 (1989).

47. Daniel, J. W., "The Approximate Minimization of Functionals." Prentice-Hall, Englewood Cliffs, NJ, 1971.

48. Cea, J., "Lectures on Minimization Problems," l'Ecole d'Eté Analyse Numérique, France, 1969; mentioned in Ref. (*47*).

49. Pike, R. W., "Optimization for Engineering Systems." Van Nostrand-Reinhold, New York, 1986.